Continuous Monitoring of Train Parameters Using IoT Sensor and Edge Computing

Yuliang Zhao, *Member, IEEE*, Xiaodong Yu, Meng Chen, Ming Zhang, Ye Chen, Xuanyu Niu, Xiaopeng Sha, Zhikun Zhan and Wen Jung Li, *Fellow, IEEE*

***Abstract*—The speed and the overall loading of a train are of great importance in determining whether the entire train is running in a safe and stable manner. We present here our work in developing a wireless rail monitoring system using IoT (Internet-of-Things) sensors and edge computing to provide accurate real-time running state parameters of trains continuously over time. By placing a wireless MEMS-based sensing system (overall size of 50×50×17 mm) on a rail to collect the vibration information of the rail under excitation by the wheels of passing trains, and by using edge computing technique to analyze these captured vibration data, we calculated the state parameters of the vehicle with the microprocessor integrated with the MEMS sensors. Then, the final analysis results were uploaded to a cloud server via Narrow Band Internet-of-Things (NB-IoT) networks. The entire system consists of a solar power module, a cloud server, and an IoT sensor. Compared with traditional train state detection systems (i.e., computer vision or IR detectors) this system has the advantages of low cost, self-powering, and no line occupation. We have demonstrated that 24-hour real-time wireless monitoring without occupation of track resources is feasible using this system, which greatly improves the efficiency and quality of railway track detection. We conducted field experiments on the Datong-Qinhuangdao Railway line using our system. Experimental results showed that the absolute error in speed is 0.2 Km/h and no error in carriages quantity detection. It is expected to play a key role in the real-time monitoring of railways and trains in the future.**

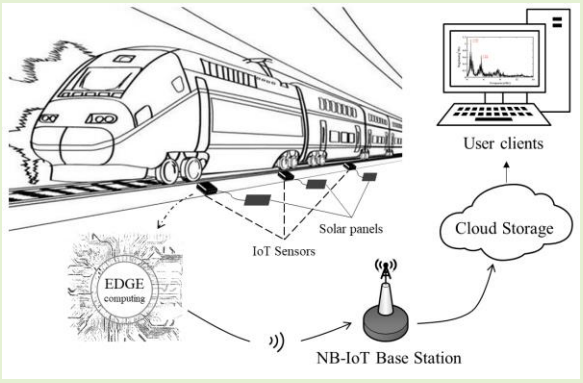

***Index Terms*—Train parameters, NB-IoT, edge computing, real-time monitoring, rail vibration**

I. Introduction

RAILWAYS is a key mass transportation method in China, i.e., the total number of passengers using train transportation in China in 2019 was about 583 times the total using air transportation [1], [2]. According to the *Railway Statistics Bulletin 2019* issued by the Ministry of Transport of the People's Republic of China, the total number of railway passenger transport in mainland China was 3.660 billion, and the total volume of railway freight was 4.389 billion metric tonnes, both increasing by more than 7% from the previous year [2]. With the increase of freight volume, railway accidents are more likely to occur, such as the catastrophic accident of front-rear collision between multiple-unit high-speed trains in Wenzhou (the "7/23 accident") [3], and derailment of trains on Jincheng line [4], resulting in a death toll of nearly 1,000 every year [5]. The safety and reliability of trains have always been the focus and difficulty of maintaining railway systems. The speed and load of the trains are important parameters to measure the safety and stability [6].

At present, besides the large track inspection car, existing railway monitoring methods are mainly divided into two types, i.e., non-contact type and contact type [7]. The difference between the two types of methods is whether there is contact between the sensing device and the track. Many non-contact methods, such as IR and cameras, have been applied to railway monitoring. Some researchers have used IR transmitter and receiver for vehicle speed and crack inspection [8] - [10]. However, IR transmitter and receiver can only identify the cracks of the rail. With the development of image processing, some researchers have adopted computer vision or image processing methods for rail monitoring [11] - [13]. As far as railway monitoring is concerned, they are effective. However, to monitor trains and rails at night, there must be high-functioning cameras, which inevitably increase the cost of

This work was supported by the National Natural Science Foundation of China (Grant No. 61873307), the Administration of Central Funds Guiding the Local Science and Technology Development (206Z1702G), the Fundamental Research Funds for the Central Universities (grant No. N2023015), Qinhuangdao Science and Technology Planning Project (201901B013), Hong Kong RGC-Joint Laboratory Funding Scheme (JLFS/E-104/18), and the Shenzhen Science and Technology Innovation Commission Municipality (grant numbers: SGDX2019081623121725).

Yuliang Zhao, Xiaodong Yu, Ming Zhang, Xuanyu Niu and Xiaopeng Sha are with the School of Control Engineering, Northeastern University at Qinhuangdao, Qinhuangdao 066004, China; Yuliang Zhao's email: (**yuxiaodongtop@163.com**.)

Zhikun Zhan is with the Lab of Industrial Computer Control Engineering of Hebei Province, School of Electrical Engineering, Yanshan University, Qinhuangdao 066004, China;

Ye Chen is with the School of Mechanical Engineering and Automation, Liaoning University of Technology, Jinzhou 121001, China;

Meng Chen and Wen J.Li are with the Department of Mechanical Engineering, City University of Hong Kong, Kowloon Tong, Hong Kong SAR, China; Wen J.Li's email: (**wenjli@cityu.edu.hk**.)

the system and consume a lot of power, not to mention the failure to realize real-time monitoring on a long-term basis.

Compared with non-contact methods, contact methods have the advantages of high precision and many detection parameters. Under a contact method, facilities along the railway, such as rails and fasteners, need to be in direct contact with the testing equipment for diagnosis and monitoring [14]. In this regard, the mainstream monitoring equipment is the track inspection car. However, this method is not only costly and time-consuming, but also requires that railway transport be stopped before detection [7]. To overcome this problem, other researchers have tried other methods such as RFID and inertial sensors. A. K. Gupta et al. [15] introduced a railcar detection system based on RFID technology for detecting train running state parameters such as path. T.X. Mei et al. [16] proposed to extract specific motion characteristics (including speed of the wheelset) from the inertial sensors mounted on the bogie frame by tracking the excitation through the dynamic response of the vehicle/bogie. This approach provides an accurate measurement of the vehicle's ground speed even in wheel slip under traction or braking. Although these methods are capable of detecting train parameters and track information, they cannot process detected data in real-time. Moreover, the testing device is not portable and the testing process is complicated, for which more time is consumed in each test.

Meanwhile, the rapid development of the Internet of Things (IoT) and the popularity of MEMS sensors provide new solutions to monitor train parameters. MEMS sensors are characterized by small size, low cost, and low power consumption. Moreover, IoT devices are capable of data processing, and hence, they can efficiently realize real-time data detection, processing, and output. David Milne et al. [17] glued a geophone and a ±16 g accelerometer to the same sleeper at a study site, where six car trains would pass by at up to 230 km/h (~60 m/s). The acceleration and velocity of the sleeper were measured to conduct a direct comparison between different data from the geophone and accelerometer, thus demonstrating the repeatability and robustness of the MEMS accelerometer under the same conditions and its potential to continuous monitoring applications. It can be seen that this kind of low-cost techniques are applicable to railway scenarios. Amin Suharjono et al. [18] used the accelerometer sensor MMA7455l to measure three-axis accelerations of a rail to detect rail vibration. Douglas Leonard Goodman et al. [19] adopted a three-axis accelerometer to detect abnormalities with the rail or train. Eugen Berlin et al. [20] reported the deployment of a wireless sensor network on railway tracks to obtain the vibration mode of 186 trains, which can be used for detecting vehicle speed, length, and other information. These methods have demonstrated the high feasibility and robustness of MEMS sensors in railway monitoring.

On the other hand, cloud computing and edge computing are widely used for processing IoT data [21]. Here, cloud computing refers to the use of a cloud server to process a large amount of data received from the terminal device through the IoT. In previous works [22], [23], we completed system construction based on micro motion sensors and used the entropy theory for detecting the looseness of rail fasteners. We analyzed the vibration data collected by the MEMS sensor in the cloud server, and determined whether fasteners would fall off through analyzing the frequency of rail vibration when a train passed by. At the same time, we conducted relevant experiments to verify the system in the detection of rail fasteners. At present, we hope to monitor vehicle speed, rail state, and other information by detecting the acceleration of rail vibration when a train passes by. However, the method based on MEMS sensors often produces a large amount of data. Assuming that our three-axis MEMS sensor has a sampling rate of 3,200 Hz and that the storage type of each data is single-precision floating point (float), the amount of data generated per second becomes 37.5 KB. The upstream rate of the wireless module (BC95-B8) is only 15.625 kbps (<38.4 kbps) [24], so it is impossible to upload all the data to the cloud server in real time. In other words, cloud computing is inapplicable to this system without replacing the wireless module.

With the rapid development of edge computing, opportunities arise for real-time railway monitoring. Edge computing is a distributed computing paradigm that brings computation and data storage closer than cloud computing to the location where it is needed, thus reducing response time and saving bandwidth [25]. Some researchers have begun to apply edge computing to real-time monitoring systems. For example, Zeba Idrees et al. [26] employed the method of edge-computing based IoT to implement air quality monitoring systems, with the purpose of reducing the computational burden of sensing nodes (reduced by 30%), and the power consumption (reduced up to 23%). In order to reduce network load and network delay of the centralized server in smart home systems, Yanqin Mao et al. [27] designed a data collection and processing scheme based on edge computing. The empirical results showed that the data acquisition and processing scheme based on edge computing could effectively reduce network communication. In addition, to monitor rails and trains on a real-time basis, Jun Guo et al. [28] proposed a large vehicle tracking method based on edge computing and feature recognition. They applied the edge device in different spatial locations, and only uploaded the feature information extracted from sensing data to the cloud server. Finally, the cloud generated the trajectory by feature matching and space-time constraint. All of these works prove that edge computing can help reduce network burden and node power consumption, and is more suitable our railway monitoring system than cloud computing.

To fully utilize the advantages of IoT sensors and edge computing, we developed a new method of combining the two techniques to realize a low-cost, low-power, wireless, and real-time rail monitoring system. In this study, we integrated sensors and microcontrollers on the circuit board to build a low-power, passive, wireless sensing device for data collection. On this basis, edge computing inside the microcontroller was performed to analyze and process the data to obtain the *speed of the train* and the *number of carriages*. At last, the measured and processed results were uploaded to the cloud server in real-time, so that users could view the train speed and carriage data directly. Compared with the non-contact method based on image processing, our developed method is superior in terms of computing speed and scene adaptation.

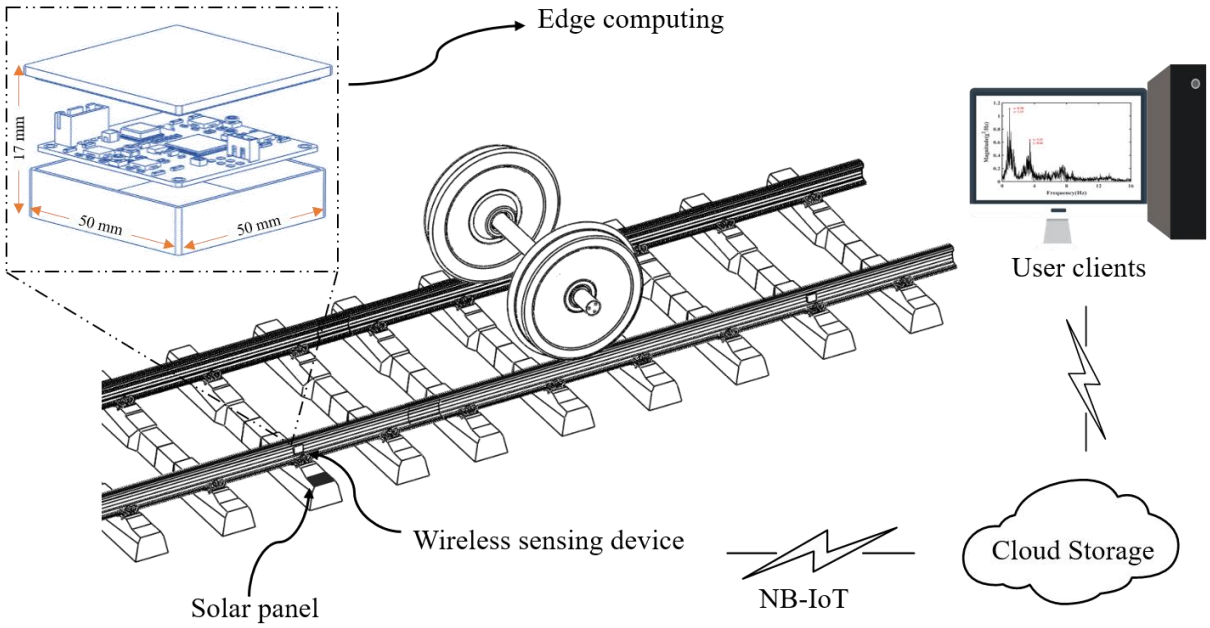

Fig. 1. System schematic diagram of real-time train monitoring based on wireless IoT sensor and edge computing.

II. System Setup

Here we detail the complete technical solution developed to build a real-time rail monitoring system based on wireless IoT sensors and edge computing. It includes system structure, experimental method, and the placement of the sensing devices.

A. System Architecture

Fig. 1 shows the general system, which consists of a wireless sensing device, a solar power module, a cloud server, and a client computer. The system is used to collect rail vibration data to determine the vehicle speed and the number of carriages by edge computing. The wireless sensing device with multiple sensors collects and processes the vibration acceleration of the rail when trains pass by. Then it sends the results to the remote cloud server via NB-IoT network. Users can view track vibration data and train parameters via user clients. Solar and lithium batteries are combined to provide uninterrupted energy for wireless sensing devices.

B. Experimental Method

We cooperated with China Railway Shanhaiguan Bridge Group Co., LTD. Our experiment was conducted at the Qinhuangdao section of the Datong-Qinhuangdao Railway line. The experimental procedures were reviewed and approved by the Qinhuangdao Public Works Section of Beijing Railway Administration, and the entire experiment was carried out with the company's personnel. The model of the train tested in the experiment was **C80B special open-top car** for coal mine, with a dead weight of 19.9 metric tonnes and a load of 80 metric tonnes. Each vehicle was 12 m in length and the train fully loaded. In order to avoid interference with neighboring railway, the sensing device should be installed as far away from the turnout as possible. Meanwhile, it was required that the rail at the sensor position be free of obvious damage, cracks, and pollutants, that fasteners be of normal tightness, that sleepers do not sink, and that the position be normal.

We chose the rail waist as the position to fix the sensing device, because it has a flat surface to smoothly contact with the side of the sensing device while keeping away from the train wheel. The first step was to confirm that no train would pass by during the installation period. Then, we cleaned the rail waist and fixed the sensor on it with strong double-sided adhesive tape. At the same time, we pasted the solar panel on the rail pillow, as shown in the scene photo in Fig. 2. Two wireless sensing devices were located close to each other to verify measured data results. In order to avoid detection errors caused by different installation positions and sensor parameters, the positioning height and orientation of the sensor were calibrated by comparison calibration. To evaluate and compare the performance consistency of the same batch of sensing devices, the sampling rate and other parameters of the sensor were kept the same.

Fig. 2. The position of two sensors and solar panels in the field experiment.

As shown in Fig. 3, the train running videos were shot by a high-speed camera in high picture quality (1920x1080@30fps), and could be used to accurately calculate vehicle speed and the cumulative number of carriages by image processing algorithm. Therefore, it can be used as a benchmark to evaluate the accuracy of the sensor detection system. Due to the adjacency to the terminal station, the train was constantly slowed down in the experiment, and the vehicle speed was set at about 30-60 km/h, which was quite different from normal freight vehicle speed (~80 km/h) [29].

Fig. 3. A train passing scene taken by a high-speed camera.

III. Platform Design

A. Sensor Development and Integration

Fig. 4(a) shows the structural block diagram of the wireless sensing device, which includes a sensing module, a data processing module, a wireless module, an orientation module, and a power supply module. Fig. 4(b) is the picture of the wireless sensing device, consisting of 1) a lithium battery, 2) a power management, 3) a microprocessor chip, 4) a MEMS accelerometer, and 5) a NB-IoT wireless transmission module. The functions of each module are described in details below. The sensing module is mainly used for data acquisition, including rail vibration acceleration and ambient temperature and humidity information; The data processing module controls the whole flow of the program, and analyzes and processes collected vibration data; The analysis results and location information obtained by the orientation module are uploaded to the cloud server via NB-IoT. The power module is used to supply suitable voltage for other modules.

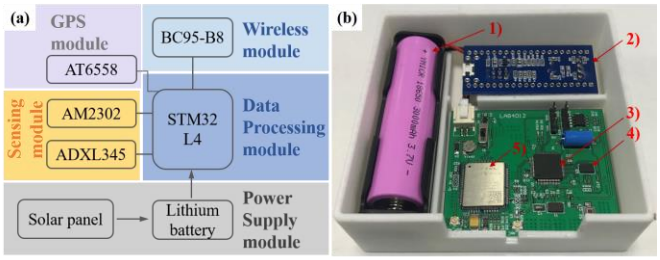

Fig. 4. (a) Structural block diagram of the wireless sensing device; (b) Picture of wireless sensing device, consisting of 1) a lithium battery, 2) a power management, 3) a microprocessor chip, 4) a MEMS accelerometer, and 5) a NB-IoT wireless transmission module.

1) Sensing Module

The sensing module includes a MEMS triaxial accelerometer and a temperature/humidity sensor. The MEMS triaxial accelerometer is used to collect the vibration information of the track, and calibrated by the temperature/humidity sensor according to collected ambient temperature and humidity. According to relevant literature, the vibration frequency of the rail is about 1,200 Hz-1,300 Hz [30]. To measure this kind of vibration, the accelerometer's measurement bandwidth should cover the frequency range. To adapt to the railway field environment and meet the design requirements of low power consumption and small size, industrial-grade devices with low power consumption and small package should be selected. Table I summarizes some specifications of three MEMS accelerometers to make a comparison of similar products. Finally, we chose the ADXL345, since its maximum measurement bandwidth of 1,600 Hz can fully meet the requirements for rail vibration detection of trains. Meanwhile, the normal operating current of ADXL345 is less than 140 μA, and its measurement range is ±16 g.

TABLE I
COMPARISON OF DIFFERENT ACCELEROMETER CHIPS

Product	Ranges (g)	Bandwidth (Hz)	Supply Current (μA)	Sensitivity (LSB/g)	Size (mm)
ADXL345	±2/±4/ ±8/±16	0.05-1,600	140	256/128/ 64/32	3×5×1
MPU6050	±1.5/±6	2-500	500	16,384/8,192/ 4,096/2,048	4×4×0.9
BMA250	±2/±4/ ±8/±16	8-1000	130	256/128/ 64/32	2×2×0.95

The ambient temperature and humidity of the rail have effect on the working performance of the detection system, so it is necessary to detect the ambient temperature and humidity. The temperature and humidity sensors need to adapt to various applications, and have the features of small size, low power consumption, and ease of integration. We selected the AM2302 digital temperature and humidity sensors (Guangzhou Aosong Electronics Co., Ltd, China), which are compound sensors with calibrated digital signal output and a temperature range of 40-80 ℃. They are characterized by small size and low power consumption.

2) Data Processing Module

The major part of the data processing module is a microprocessor chip. In addition to requiring low power consumption, the microcontroller controls the overall process of the whole sensor, and carries out edge computing. Therefore, sufficient operation speed and sufficient storage space are also required. Table II summarizes the specifications of three commercial microprocessor products with similar performance.

TABLE II
COMPARISON OF DIFFERENT MICROPROCESSOR CHIPS

Company	Product	Performance (DMIPS/ MHz)	Power Consumption (@80MHz)	Flash (KB)	Budgetary Price ($)
STMicroelectronics	STM32L476RGT6	1.25	8 mA	1, 024	4.3167
STMicroelectronics	STM32F407VET6	1.25	40 mA	512	4.7724
Texas Instruments	TM4C1294KCPDT	1.25	76mA	512	5.40

The STM32L4 series not only has enough peripheral interfaces and 2.0 V to 3.6 V working voltage range compatible with mainstream battery technology, but also breaks the performance limit in the field of ultra-low power consumption. We chose STM32L476RGT6 from ST company, because of its low power consumption (100 μA/MHz) and sufficient flash space (1MB). It delivers 100 DMIPS based on its Arm® Cortex®-M4 core with FPU and ST ART Accelerator™ at 80 MH (1.25 DMIPS/MHz), which can meet our test requirements [31].

3) *Wireless Module*

In this paper, we used the data processing module for the edge computing of the data collected by the accelerometer, and uploaded preliminary results to the cloud server. So for the wireless communication module, the amount of data transmitted each time is not large, and intermittent transmission is sufficient. This creates a lot of advantages, such as reducing the overall power consumption, improving the monitoring time, and easing the burden on the microprocessor and wireless communication module. Therefore, the wireless module to be selected must, first of all, have a sleep mode. At the same time, power consumption should be low in both the transmission process and the sleep mode. In addition, small size and long-distance transmission should also be a focus of consideration. Table III compares the power consumption of typical LPWAN and WWAN communication modules. We selected the high-performance and low-power NB-IoT wireless communication module (BC95-B8) from the table, because it is designed with both sleep mode (with a current of 3 μA only) and power-saving mode (with a current of 0.5 mA). Meanwhile, its size is only 23.6 mm × 19.9 mm × 2.2 mm.

TABLE III
COMPARISON OF DIFFERENT COMMUNICATION MODULE CHIPS

	Product	Sleep Mode (μA)	Sleep Mode (mA)	Receive (mA)	Transmit (mA)	Size (mm)
LPWAN						
NB-IoT	BC95-B8	3	0.5	60	70(0dbm) 130(12dbm) 230(23dbm)	23.6×19.9 ×2.2
WWAN						
GSM/ GPRS	SIM800C	800	12.8	267(DCS1800,1Rx,4Tx) 204(DCS1800,3Rx,2Tx) 147(DCS1800,4Rx,1Tx)		17.6×15.7 ×2.3

4) *Other Modules and Components*

In order to quickly locate each sensing device, we integrated a GPS module into each sensing device. The AT6558 series satellite positioning chip encapsulated by QFN40 is adopted for the GPS module with a size of 5 mm × 5 mm × 0.8 mm only. The chip supports single system positioning of GPS/ BDS/ GLONASS satellite navigation system, or multi-system joint positioning of any combination. Its standby power consumption is lower than 10 μA, and dual-mode continuous operation current is as low as 23 mA, which can outperform similar products.

In order to achieve 24-hour continuous monitoring, the power supply module is designed with two parts: solar panel and rechargeable lithium battery. In consideration of the volatility of solar illumination, the wireless sensing device is powered by the rechargeable lithium battery (1,300 mAh). Table IV summarizes the typical power consumption of the components in the proposed wireless sensing device. The total power consumption of the sensing device is about 670 mWh/day (3.3 V). Therefore, the 1,300 mAh lithium battery can power the device for six consecutive days, even without the solar panel. For the purpose of ensuring the continuous and stable operation of the device, a solar panel is installed to add power to lithium battery. Taking into account issues such as lighting time and irradiation angle, the solar panel (117 mm×136 mm) can generate electrical power at the rate of about 1,700 mWh (3.3 V)/d (five hours under normal light). In other words, it takes about 2 days to fully charge the 1,300 mAh lithium battery, and the energy generated by the solar panel can be used by the wireless sensing device for more than two days.

TABLE IV
TYPICAL POWER CONSUMPTION OF THE WIRELESS SENSING DEVICE PROPOSED IN THIS PAPER

	Min. (mW)	Typ. (mW)	Max.(mW)
Data Processing Module			
Microprocessor run	/	26.7(@80MHz)	33(@80MHz)
Microprocessor sleep	/	0.0033	0.0066
ADC	/	3.6 (16 bits)	/
Sensor			
Acceleration	/	0.462	/
Temperature/Humidity	3.3 (working) 1.65 (idle)	/	3.3 (working) 1.65 (idle)
Orientation Module	/	76.7	/
Wireless Module			
Tx Power (0 dbm)	/	231	294
Tx Power (12 dbm)	/	429	546
Rx Power	/	198	252

In addition, we have a 64g SD card on the device to store the raw data of high sampling rate (3,200 Hz) collected by the accelerometer. The raw data is used to verify the results of microprocessor edge computing and for subsequent data mining.

B. *Train Parameter Extraction Algorithm*

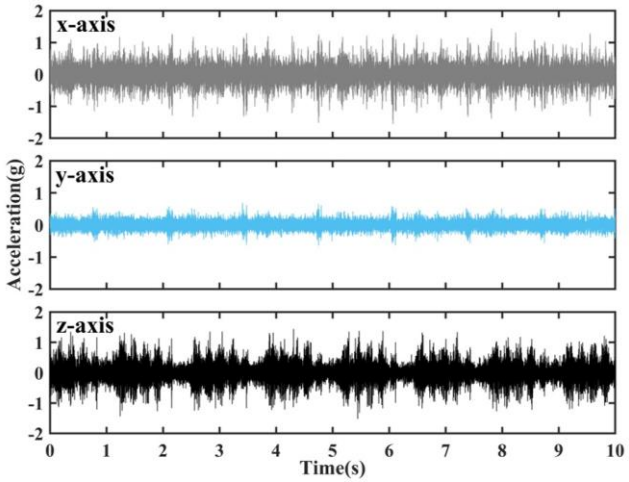

Fig. 5. Raw data of triaxial acceleration generated by track vibration when a train passed by.

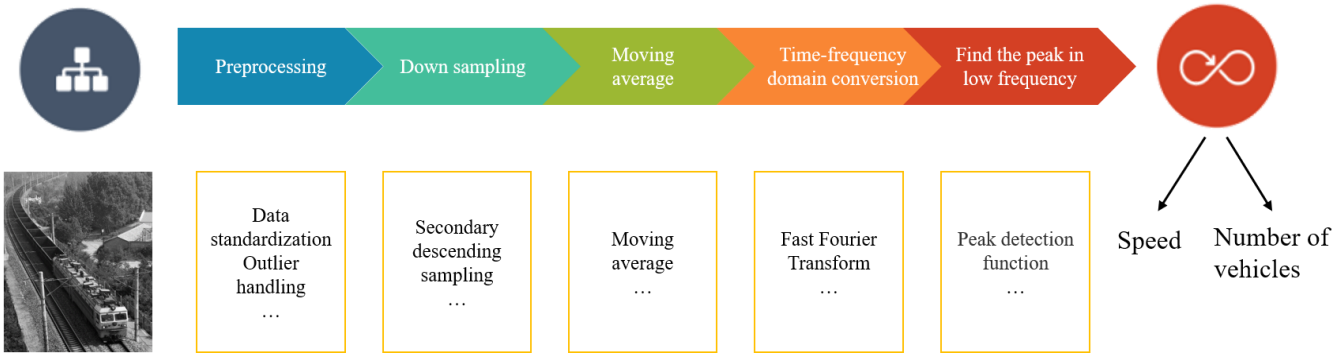

Fig. 6. Procedure of calculating train state parameters based on z-axis acceleration data.

Fig. 5 shows the triaxial original data of acceleration generated by track vibration when 25 carriages passed by the sensor. It can be clearly seen that the z-axis acceleration is obviously periodic, and that the triaxial accelerations are highly correlated. Therefore, we used the z-axis acceleration for analysis.

Fig. 6 shows the procedure of calculating train state parameters based on the original z-axis acceleration data, mainly including the preprocessing, descending sampling, moving average, and time-frequency domain transformation of the original acceleration data. Finally, we acquired the train running state parameters by extracting the frequency domain characteristics of the signal. In order to facilitate the subsequent evaluation and analysis of the detection results, the pre-processed acceleration data were stored in the SD card for backup.

1) *Data Pre-processing, Secondary Sampling, and Moving Average*

High-sampling rate raw data collected by MEMS accelerometers often have noises and outliers. The outliers in the data deserve attention, as it is very dangerous to ignore them. Introducing outliers into calculation and analysis will have an adverse impact on the results. The purpose of data preprocessing is to remove outliers and the data standardization target zone [32]. We used the box-plot to define the upper and lower bounds of the outliers. The first step was to determine the upper and lower quartiles in the data. The upper quartile is defined as U and the lower quartile as L. Then, the difference between them is defined as IQR. In the final step, we calculated the upper and lower bounds of the data, defined as MAX and MIN, respectively. MAX and MIN are estimated as:

$$MAX = U + 1.5 \times IQR \tag{1}$$

$$MIN = L - 1.5 \times IQR \tag{2}$$

where MAX denotes the upper limit, and MIN the lower limit. After removing the outliers, we converted the preprocessed data into the standard unit g, as shown in Fig. 7(a). Apparently, the data has a certain periodicity.

Literature survey shows that vibration above 400 Hz is dominated by rail, and that the maximum acceleration of rail vibration occurs near 1,300 Hz, which is the first-order bending resonance frequency of the rail supported by the foundation under the rail. According to Shannon's sampling theorem, our acceleration sampling frequency should be at least 2,600 Hz to perfectly capture rail vibration. To analyze more frequency components and get useful information from the raw data, we set the sampling rate of the sensor to 3,200 Hz. But, obviously, the microprocessor cannot analyze the large amount of data with a sampling rata of 3,200 Hz. In addition, the detection of vehicle speed and cumulative number of passed carriages can be determined by the time interval between two adjacent carriages [33], [34]. Therefore, we stored the raw data with a sampling rate of 3,200 Hz into the SD card, and then reduced the sampling rate to 32 Hz to analyze the vehicle speed and the cumulative number of passed carriages.

Here we used the method of moving average to pre-process and filter the raw data. Assuming input as x and output as y, the calculation formula of N moving average filtering is:

$$y = \frac{1}{N}\sum_{i=0}^{N-1} x_{N-i} \tag{3}$$

The data after applying a 100 moving average filter is shown in Fig. 7(b).

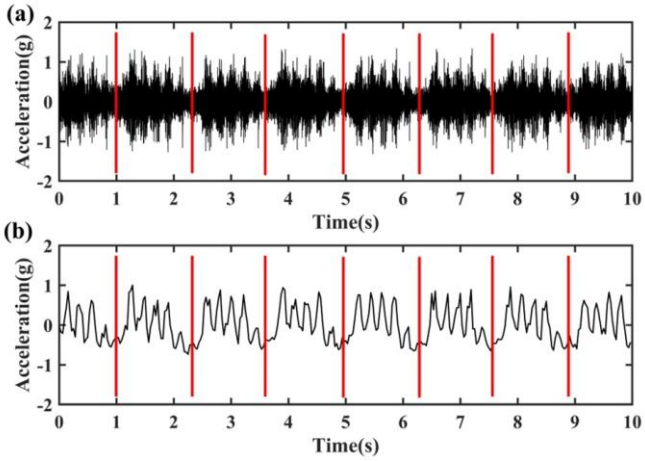

Fig. 7. (a) Z-axis acceleration after preprocessing, where the data between two adjacent red lines (window size 1.28 s) is the vibration acceleration caused by the passing of a train; (b) Z-axis acceleration data after secondary sampling and moving average.

2) *Time Domain - frequency Domain Transformation*

In order to simplify the calculation, the acceleration signal after 32 Hz subsampling is transformed from time domain to frequency domain for analysis. Frequency domain analysis can decompose complex signals into simple superpositions of sinusoidal signals, and accurately describe signals with limited

parameters [35]. Fast Fourier Transform (FFT), characterized by low complexity of computing, has been widely applied in signal processing. The principle of FFT algorithm is implemented by many small and simple transformations, instead of large-scale transformation, to reduce operation requirements and improve operation speed. The FFT results of data in Fig. 7(b) are drawn as the spectrogram in Fig. 8.

There are two obvious peaks of the magnitude in Fig. 8. The frequency of the first magnitude peak (0.78 Hz) reflects the vibration induced by the carriages, which is coincide with the frequency obtained by our infield measurement. The other frequency of magnitude peak (3.21 Hz) is induced by the wheels. Each carriage is composed of four pairs of wheels. Therefore, the vibration frequency caused by the passing of the wheels is about four times of that caused by the passing of the carriages.

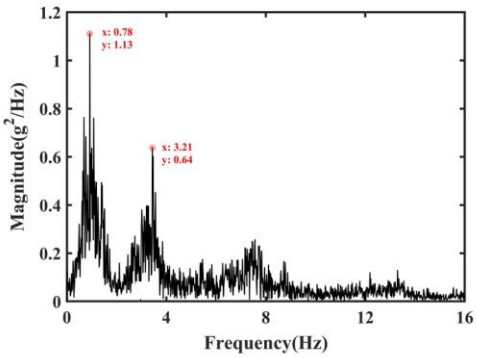

Fig. 8. The spectrum of the low frequency band when a train passed by, where the frequency (0.78 Hz) of first magnitude peak is induced by the carriages, and another frequency (3.21 Hz) of magnitude peak is caused by the wheels.

3) *Methods of Calculating Vehicle Speed and the Cumulative Number of Carriages*

When a train is running, its speed is an important parameter [36], and also an important metric evaluating whether the train in service is safe and stable. In order to improve the efficiency of the line transportation and ensure the safety of the train, it is necessary to monitor train speed while increasing train load.

When a train is running on track, its wheels produce high-amplitude vibration signals at the contact position, shown as periodic peak and trough characteristics in the time domain acceleration waveform. Each carriage generates such a peak that the period equals to the time of the carriage passing by the sensing point on the rail. The length of the carriage divided by the period is the running speed of the train. In addition, these peaks and trough features can be superimposed by sinusoidal waves of different frequencies and amplitudes. In the frequency domain, each sinusoidal wave decomposed in the time domain corresponds to a frequency in the frequency domain, namely, the horizontal axis is the frequency and the vertical axis the amplitude of the frequency signal. In order to calculate the speed of a vehicle, the frequency at which the vehicle passes by the detection point needs to be found in the low-frequency band. According to relevant regulations, the maximum running speed of the train on Datong-Qinhuangdao Railway line is no more than 80 Km/h, and the standard length of the carriage is 12 m, so the frequency of the carriage passing by the detection point is no more than 2.32 Hz. For this consideration, this paper chooses a range of 0-2.5 Hz to search for the peak value.

We used a dedicated library for the microcontroller provided by STMicroelectronics for FFT analysis. The number of acceleration readings to complete the FFT should be 2^n (n should be less than or equal to 10) [37]. If n is set to 10, the original data size shall be 100×2^{10}. The complexity of the algorithm designed in this paper is O(N*logN), and it takes about 15,360 instructions to complete an operation. According to the operation speed (100 DMIPS) of the microprocessor provided by ST Company [31], the microprocessor can complete the operation within the 15.36 ms without delay. Since the sampling rate of the sensor is 3,200 Hz, it takes 32 seconds to collect these data. This is the time required for data accumulation before train parameters can be calculated. In the subsequent data processing tasks, 32 seconds is taken as the width of the time window, and sliding and translation are performed on the data axis at an interval of five seconds to realize repeated calculation of train parameters. For this reason, vehicle speed and the cumulative number of carriages in the past 32 seconds are calculated every five seconds.

According to Fig. 8 and Fig. 9, the frequency corresponding to the peak at 32 seconds is 0.78 Hz. In other words, the average frequency of train cars passing by the target sensing device in the data accumulation stage is 0.78 Hz. According to:

$$v = l \times f \tag{4}$$

the average speed of the train within 32 seconds is 31.696 Km/h. Since we have determined the time required for a car to pass by the target sensing device completely, we can roughly calculate the number of cars to pass by during this period from:

$$n = 32 \times f \tag{5}$$

As the Datong-Qinhuangdao Railway line uses professional tracks for fully loaded vehicles heading to Qinhuangdao Station, detecting the cumulative number of carriages will be favorable for judging the accumulated traffic and analyzing rail life.

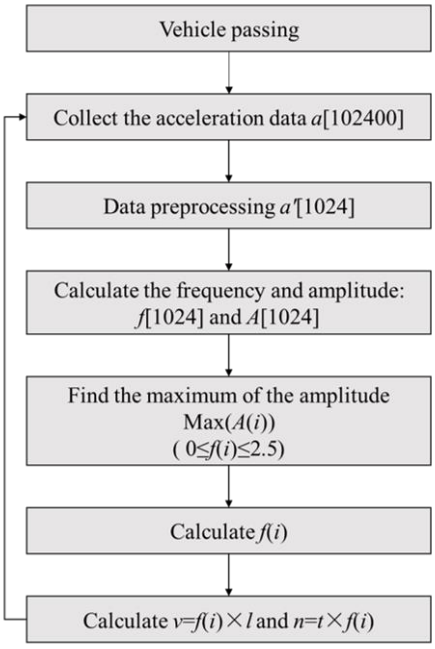

Fig. 9. Procedure of computation by a microprocessor.

IV. Results and Analysis

In this section, we present and verify experimental results, and evaluate the performance of the whole hardware and algorithm. One or more wireless sensing devices are placed on the rail waist to collect track vibration acceleration during train operation. The devices process the acceleration data, and upload the results to the cloud. In addition, we have also installed a high-speed camera on the slant of the track to record the train operation and verify the reliability of the algorithm.

1) *Verification of Vehicle Speed and the Number of Carriages*

In the experiment, the vehicle speed and the number of carriages obtained from the video taken by the high-speed camera are considered as true values. We compared the results of the microprocessor calculation, the results of the offline calculation of the data in the SD card, and the true values, as shown in Fig. 10(a). Black spots are the true value of speed obtained by the video taken by the high-speed camera; blue spots and red spots are the train speeds calculated by raw data (offline 3,200 Hz) and edge computing (online 32 Hz), respectively. Blue line and red line are the number of carriages calculated by raw data (offline 3,200 Hz) and edge computing (online 32 Hz), respectively; black line is the true value of the cumulative number of carriages obtained by the video taken by the high-speed camera.

According to further analysis, the absolute error of the vehicle speeds from edge computing and true value was within 0.2 km/h, while the error between raw data and true value was within 0.15 Km/h. In addition, the number of passing carriages from the raw data (offline 3,200 Hz) and edge computing (online 32 Hz) were both correct.

2) *Monitoring of the Total Transport Volume and Number of Carriages Within 24 Hours*

For Datong-Qinhuangdao Railway line, we counted the total transport volume and the number of carriages within 24 hours, as detailed in Fig. 10(b). The blue line represents total transport volume and the red line represents the number of carriages. The curve rising represents a train passing by, and different slopes represent different speeds.

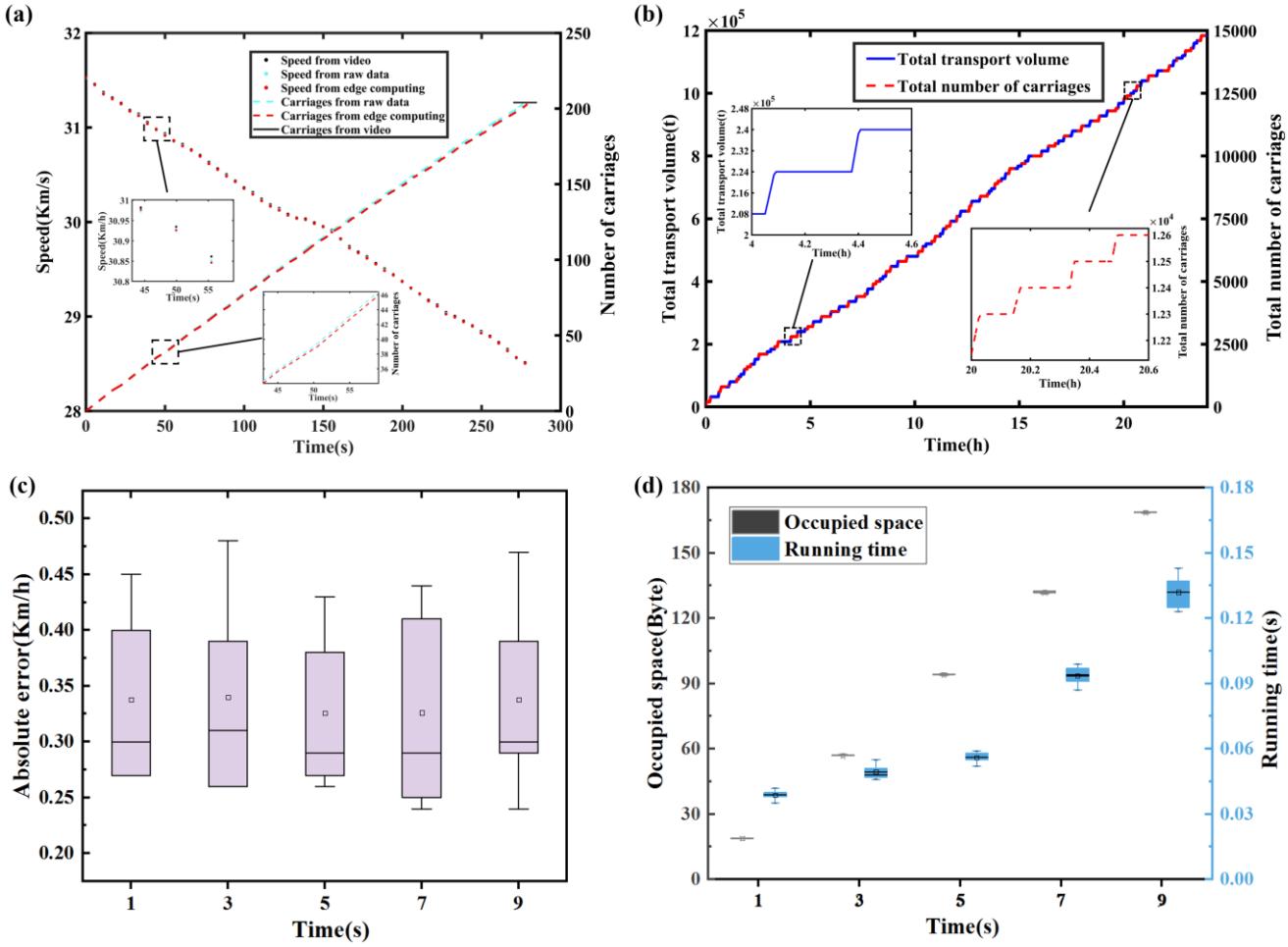

Fig. 10. (a) Comparison of train speeds and number of carriages calculated by video, raw data, and edge computing, among them black spots are the true value of speed obtained by the video taken by the high-speed camera; blue spots and red spots are the train speeds calculated by raw data (offline 3,200 Hz) and edge computing (online 32 Hz), respectively; blue line and red line are the number of carriages calculated by raw data (offline 3,200 Hz) and edge computing (online 32 Hz), respectively; black line is the true value of the cumulative number of carriages obtained by the video taken by the high-speed camera; (b) Total transport volume and total number of carriages measured by the real-time rail monitoring system within 24 hours; (c) Boxplot comparison of the absolute errors of five intervals; (d) Boxplot comparison of the running time and the occupied space of five intervals.

According to the results, 92 trains with C80B special open wagons for coal transport passed by within 24 hours, with 15,096 carriages in total. The cumulative coal transport capacity in one day was more than 1.2 million tons, or more than 50,000 tons per hour on average. Then the annual coal transport capacity of this railway would exceed 400 million tons, consistent with the annual coal transport capacity of Datong-Qinhuangdao Railway line [38]. This fully proves the reliability and accuracy of the system and method.

3) *Method of Evaluation*

As mentioned in the part about calculating vehicle speed and the cumulative number of carriages using edge computing, sliding and translation were performed on the sensor readings every five seconds. We evaluated the different intervals by three metrics, i.e., accuracy, running time, and occupied space. Fig. 10(c) shows the boxplot of the absolute error of the vehicle speed at five intervals. Clearly, an interval of five seconds was more stable than other intervals. In addition, Fig. 10(d) shows the boxplot of the running time and occupied space at five intervals. With the increase of time interval, the running time and the occupied space both significantly increased. Considering all the three metrics, we chose five seconds as the interval.

V. Discussion

As presented above, we have verified the feasibility of applying our system to the detection of vehicle speed and the cumulative number of carriages. During the experiments, we found that the impact of algorithm complexity on the processing time and memory space of the microprocessor is very critical. One limitation of this study lies in that only a FFT algorithm was used in the edge computing of the microprocessor, which requires a long time of data accumulation and a large amount of data buffer space. This caused a waste of microprocessor resources and increased the power consumption of the sensing system. Therefore, in the future, we will select a more suitable microprocessor and integrate intelligent algorithms with reduced computational burden into the edge computing process.

Another limitation of this study is that the experiments were done on freight railways. However, for commercial applications, the monitoring of passenger railways is also very important. Therefore, in the future we will verify the universality of this system through a large number of experiments on passenger railways. We envision that this system will also be used to monitor other important components in the railway, e.g., turnouts, sleepers, etc..

VI. Conclusion

In this paper, we presented a train rail monitoring framework to provide train speed and number of carriages information based on IoT sensors and edge computing technologies. In our scheme, the sensing system is placed at the rail waist to collect the rail vibration acceleration caused by passing trains. Edge computing is carried out by the microprocessor in the sensing system, and real-time results are uploaded to the Cloud. For the hardware design, we have implemented a wireless sensing device that integrates accelerometer and microprocessor to detect and analyze the vibration of the rail. The sensing system is also integrated with a solar panel for continuous operations over time. Computationally, the time-domain accelerations are converted into the frequency domain to identify the running speed of the train and the number of carriages. As indicated by experimental results, this method accurately recognizes the speed and the number of carriages of the moving train, and the stability of the entire system is verified. Finally, we demonstrated that this scheme is capable for 24-hour real-time monitoring without occupation of track resources, which greatly enriched the detection method of railway operation status.

Acknowledgment

This work was supported by the National Natural Science Foundation of China (Grant No. 61873307), the Administration of Central Funds Guiding the Local Science and Technology Development (206Z1702G), the Fundamental Research Funds for the Central Universities (grant No. N2023015), Qinhuangdao Science and Technology Planning Project (201901B013), Hong Kong RGC-Joint Laboratory Funding Scheme (JLFS/E-104/18), and the Shenzhen Science and Technology Innovation Commission Municipality (grant numbers: SGDX2019081623121725).

References

[1] Civil Aviation Administration of China, “2019 Civil Aviation Industry Development Statistical Bulletin,” Civil Aviation Administration of China, 2020. http://www.caac.gov.cn/XXGK/XXGK/TJSJ/202006/t20200605_202977.html (accessed Jul. 13, 2020).

[2] National Railway Administration of the People’s Republic of China, “2019 Statistic Bulletin of China Railway Corporation,” National Railway Administration of the People’s Republic of China, 2020. http://www.nra.gov.cn/xxgkml/xxgk/xxgkml/202004/t20200430_107575.html (accessed Jul. 13, 2020).

[3] Y. Zhou, X. Tao, L. Luan, and Z. Wang, “Safety justification of train movement dynamic processes using evidence theory and reference models,” Knowledge-Based Syst., vol. 139, pp. 78–88, Jan. 2018.

[4] Shenyang Railway Administration, “Announcement on investigation and handling of major traffic Accident of Passenger Train derailment on Jincheng Line ‘4.12,’” Shenyang Railway Administration, 2020. http://www.nra.gov.cn/xxgkml/xxgk/xxgkml/202004/t20200430_107578.html (accessed Jul. 13, 2020).

[5] National Railway Administration of the People’s Republic of China, “Railway Safety Situation Notice 2019,” National Railway Administration of the People’s Republic of China, 2020. http://www.nra.gov.cn/jgzf/zfjg/zfdt/202003/t20200327_107025.shtml (accessed Jul. 13, 2020).

[6] J. Zhao-yuan, “Research on train safety monitoring expert system,” J. China Railw. Soc., vol. 22, no. 5, pp. 24–27, 2000.

[7] O. Yaman, M. Karakose, and E. Akin, “Improved Rail Surface Detection and Condition Monitoring Approach with Improved Rail Surface Detection and Condition Monitoring Approach with FPGA in Railways,” in International Conference on Advanced Technology & Sciences (ICAT’17), 2017, pp. 108–111.

[8] R. V Pise and P. D. Nikhar, “Review on Railway Track Crack Detection Using Ir Transmitter and Receiver,” Int. Res. J. Eng. Technol., vol. 4, no. 1, pp. 1723–1726, 2017, [Online]. Available: https://irjet.net/archives/V4/i1/IRJET-V4I1343.pdf.

[9] B. S. R. Krishna, D. V. S. Seshendra, G. G. Raja, T. Sudharshan, and K. Srikanth, “Railway Track Fault Detection System by Using IR Sensors and Bluetooth Technology,” Asian Iournal Appl. Sci. Technoligy, vol. 1, no. 6, pp. 82–84, 2017.

[10] P. Lad and M. Pawar, “Evolution of railway track crack detection system,” 2016 2nd IEEE Int. Symp. Robot. Manuf. Autom. ROMA 2016, pp. 1–6, 2017.

[11] H. Trinh, N. Haas, Y. Li, C. Otto, and S. Pankanti, "Enhanced rail component detection and consolidation for rail track inspection," Proc. IEEE Work. Appl. Comput. Vis., pp. 289–295, 2012.
[12] S. Faghih-Roohi, S. Hajizadeh, A. Nunez, R. Babuska, and B. De Schutter, "Deep convolutional neural networks for detection of rail surface defects," Proc. Int. Jt. Conf. Neural Networks, vol. 2016-Octob, pp. 2584–2589, 2016.
[13] M. Karakose, O. Yaman, M. Baygin, K. Murat, and E. Akin, "A New Computer Vision Based Method for Rail Track Detection and Fault Diagnosis in Railways," Int. J. Mech. Eng. Robot. Res., vol. 6, no. 1, pp. 22–27, 2017.
[14] S. Chang, Y. S. Pyun, and A. Amanov, "Wear enhancement of wheel-rail interaction by ultrasonic nanocrystalline surface modification technique," Materials (Basel)., vol. 10, no. 2, pp. 188, 2017.
[15] A. K. Gupta, "Railway Track Finding System with RFID Application," Int. J. Comput. Appl., vol. 83, no. 7, pp. 24–30, 2013.
[16] T. X. Mei and H. Li, "A novel approach for the measurement of absolute train speed," in Vehicle System Dynamics, 2008, vol. 46, no. Suppl.1, pp. 705–715.
[17] D. Milne et al., "Proving MEMS Technologies for Smarter Railway Infrastructure," Procedia Eng., vol. 143, pp. 1077–1084, 2016.
[18] A. Suharjono, E. D. Wardihani, Y. Febryana, and K. Hardani, "Analysis Of The Vibration Signal Detection For Rail Train Arrival," in 2017 IEEE International Conference on Communication, Networks and Satellite (Comnetsat) Analysis, 2017, pp. 85–87.
[19] D. L. Goodman, J. Hofmeister, and R. Wagoner, "Advanced diagnostics and anomaly detection for railroad safety applications: Using a wireless, IoT-enabled measurement system," in AUTOTESTCON (Proceedings), Dec. 2015, vol. 2015-December, pp. 273–279.
[20] E. Berlin and K. Van Laerhoven, "Sensor networks for railway monitoring: Detecting trains from their distributed vibration footprints," in Proceedings - IEEE International Conference on Distributed Computing in Sensor Systems, DCoSS 2013, 2013, pp. 80–87.
[21] A. V. Dastjerdi and R. Buyya, "Fog Computing: Helping the Internet of Things Realize Its Potential," Computer (Long. Beach. Calif)., vol. 49, no. 8, pp. 112–116, 2016.
[22] H. Sun et al., "Looseness Detection of Rail Fasteners Using MEMS Sensor and Power Spectrum Entropy," in 2018 IEEE 1st International Conference on Micro/Nano Sensors for AI, Healthcare, and Robotics, NSENS 2018, 2018, pp. 25–29.
[23] Z. Zhan et al., "Wireless Rail Fastener Looseness Detection Based on MEMS Accelerometer and Vibration Entropy," IEEE Sens. J., vol. 20, no. 6, pp. 3226–3234, 2020.
[24] E. Temperature, C. Size, Q. Enhanced, M. Serial, E. Internet, and S. Protocols, "Quectel BC95-G Multi-band NB-IoT Module with Ultra-low Power Consumption," pp. 19–20, 2019.
[25] E. Hamilton, "What is Edge Computing: The Network Edge Explained," cloudwards.net., 2019. .
[26] Z. Idrees, Z. Zou, and L. Zheng, "Edge computing based IoT architecture for low cost air pollution monitoring systems: A comprehensive system analysis, design considerations & development," Sensors (Switzerland), vol. 18, no. 9, pp. 3021, 2018.
[27] Y. Mao, J. Y. Mao, Z. Wu, and S. Shen, "A Data Acquisition and Processing Scheme Based on Edge Calculation," in the 8th International Conference on Computer Engineering and Networks (CENet2018), 2018, vol. 905, pp. 216–222.
[28] J. Guo, Y. Ma, D. Gao, B. Wang, X. Liu, and Y. Liu, "Large vehicle trajectory tracing method based on edge calculation," in ACM International Conference Proceeding Series, 2018, pp. 1–6.
[29] Z. Dou, "Study on China Heavy-haul Railway Target Speed," vol. 60, no. 4, pp. 10–13, 2016.
[30] K. Wang, "Analysis of Random Vibration Chracteristics and Verification of Track Sructrue on Frequency Domain Method," Chinese J. Mech. Eng., vol. 41, no. 11, pp. 149, 2005.
[31] STM32L476 Datasheet, Geneva, Switzerland.
[32] C. B. Royeen, "The Boxplot: A Screening Test for Research Data," Am. J. Occup. Ther., vol. 40, no. 8, pp. 569–571, 1986.
[33] S. Ni, Y. Huang, and K. Lo, "Computers and Geotechnics An automatic procedure for train speed evaluation by the dominant frequency method," Comput. Geotech., vol. 38, no. 4, pp. 416–422, 2011.
[34] S. J. Ã, H. Lin, and J. Huang, "Dominant frequencies of train-induced vibrations," J. Sound Vib., vol. 319, pp. 247–259, 2009.
[35] G. I. Redford and R. M. Clegg, "Polar plot representation for frequency-domain analysis of fluorescence lifetimes," J. Fluoresc., vol. 15, no. 5, pp. 805–815, 2005.
[36] D. R. M. Milne, L. M. Le Pen, D. J. Thompson, and W. Powrie, "Properties of train load frequencies and their applications," J. Sound Vib., vol. 397, pp. 123–140, 2017.
[37] J. Markel, "FFT pruning," IEEE Trans. Audio Electroacoust., vol. 19, no. 4, pp. 305–311, 1971.
[38] L. Shao, Y. Li, and Y. Chen, "Research on noise characteristics and control technology of heavy haul railway in China," IOP Conf. Ser. Earth Environ. Sci., vol. 300, no. 3, pp. 032050, 2019.

YULIANG ZHAO received his B. S. degree in mechanical engineering from the Hubei University of Automotive Technology, his M.S. degree in mechanical engineering from Northeastern University, and his Ph.D. degree in mechanical and biomedical engineering from the City University of Hong Kong, Hong Kong, in 2016. He is currently an assistant professor at the Northeastern University at Qinhuangdao, China. His research interests include intelligent sensors, machine learning, motion analytics, and big data analyses; his recent work involves applying these technologies to single-cell and biomechanical analyses.

XIAODONG YU received his B.S. degree in automation from Dalian Minzu University in 2017, his M.S. degree in the School of Control Engineering, Northeastern University at Qinhuangdao, China. He is currently pursuing an M. S degree in control engineering at the Northeastern University at Qinhuangdao, China. His research interests include intelligent wearable devices, inertial measurement unit, and cyber physical systems.

MENG CHEN received the B.S. degree in software engineering from Shenzhen University, Shenzhen, China, in 2009. He is currently pursuing the Ph.D. degree at the City University of Hong Kong, Hong Kong. He was a Research Assistant with the City University of Hong Kong, Shenzhen Research Institute, Shenzhen, China, from 2013 to 2015, the City University of Hong Kong from 2015 to 2016, and the Shenzhen Academy of Robotics, Shenzhen, from 2016 to 2017. His current research interests include wireless sensor networks, network transmission protocols, and artificial intelligence.

MING ZHANG received his B.S. degree in Electrical engineering and automation from North China University of Science and Technology in 2018. He is currently pursuing an M. S degree in control engineering at the Northeastern University at Qinhuangdao, China. His research interests include intelligent wearable devices, inertial measurement unit, and Machine learning.

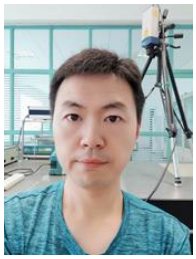

YE CHEN received the B.S. and M.S. degree in mechanical design and theory from Northeast Agricultural University in 2007 and 2010, respectively, He received the Ph.D. degree in mechanical design and theory from Northeastern University in 2020. He works at the Institute of Vibration Engineering, Liaoning University of Technology at Jinzhou, China. His research focuses on vibration utilization and control, which includes utilization of ultrasound vibration, micro ultrasonic motor, modeling and analysis of linear or nonlinear vibrations, and vibration control of mechanical systems.

XUANYU NIU is a third-year undergraduate student in the School of Control Engineering, Northeastern University at Qinhuangdao, China. His research interests include 3D modeling, 3D printing, finite element analysis, dynamic simulation and metal processing. He is currently working on embedded systems, data collation of rails, and indoor positioning systems.

XIAOPENG SHA received her B. S. degree from the Department of Information Engineering from Tangshan College, and her Ph. D. degree from the School of Electrical Engineering from Yanshan University, China. She is currently a lecturer in the Northeastern University at Qinhuangdao, China. Her research interests include micro visual serving, microrobotic systems, and intelligent sensors.

ZHIKUN ZHAN received her B. S. degree in automation from Hebei Normal University and her Master's and PhD degrees in engineering from the Shenyang Institute of Automation, Chinese Academy of Sciences. She is currently an associate professor in the School of Electrical Engineering, Yanshan University at Qinhuangdao, China. Her research interests include intelligent sensors, microfluidic chips and bio-medicine sensors.

WEN J. LI (F'11) received his B. S. and M. S. degrees in aerospace engineering from the University of Southern California (USC), in 1987 and 1989, respectively, and his Ph. D. degree in aerospace engineering from the University of California, Los Angeles (UCLA), in 1997. He is currently a chair professor in the Department of Mechanical Engineering, and concurrently serving as Associate Provost of the City University of Hong Kong. From September 1997 to October 2011, he was with the Department of Mechanical and Automation Engineering, The Chinese University of Hong Kong. His industrial experience includes the Aerospace Corporation (El Segundo, CA), NASA Jet Propulsion Laboratory (Pasadena, CA), and Silicon Microstructures, Inc. (Fremont, CA). His current research interests include intelligent cyber physical sensors, super-resolution microscopy and nanoscale sensing and manipulation. Dr. Li is an IEEE Fellow and served as the President of the IEEE Nanotechnology Council in 2016 and 2017.